Detection Characteristics Error Performance analysis of High-speed Optical PPM Communication Systems with an SNSPD

Ziyuan Shi[1,2], Xiaowei Wu[1], Lei Yang[1], Yueying Zhan[1], and Theodoros A. Tsiftsis[3]
[1]Technology and Engineering Center for Space Utilization, Chinese Academy of Sciences, China
[2]University of Chinese Academy of Sciences, China
[3]University of Thessaly, Greece
E-mail: {shiziyuan18, wuxiaowei, yang.lei, zhanyueying}@csu.ac.cn , tsiftsis@uth.gr

***Abstract*—In this paper, we investigate high-speed optical wireless communication systems that use pulse-position-modulation (PPM) and superconducting nanowire single-photon detectors (SNSPDs). We focus on scenarios where the dead time of the SNSPD is longer than a PPM symbol time. To estimate the photon detection probability for each PPM time slot, we utilize Markov chain analysis. Our findings show that the photon detection probability increases with the index of PPM time slot, meaning that the PPM time slot at the end of the symbol has a higher photon detection probability than that at the beginning of a PPM symbol. Using this probability, we derive closed-form expressions for the symbol error rate and channel coding rate of laser PPM systems. We validate our theoretical analysis with Monte-Carlo simulation results. Additionally, we show that optimizing the code rate of channel coding is possible by taking into account the order of PPM and the optical power received at the receiver.**

***Index Terms*—superconducting nanowire single-photon detectors (SNSPDs), Markov chain, Deep space communication systems**

I. Introduction

In the past two decades, laser communications have received considerable attentions in both near-earth and deep-space explorations for the massive bandwidth [1]. In deep-space tasks, laser communications with pulse-position-modulation (PPM) and photon-counting receivers are commonly considered due to the high energy efficiency [2]–[4]. Theoretically, it has been proved in [5]–[8] that a laser communication system with PPM and ideal photon-counting detectors can attain a substantially higher sensitivity than that with traditional detectors and modulation formats.

Regarding photon-counting detectors, there are a few common types including superconducting nanowire singlephoton detector (SNSPD), single-photon avalanche photodiode (SPAD), transition edge sensor (TES), photomultiplier tube (PMT), and others. In practice, photon-counting detectors are not ideal as they have parasitic effects such as dark counts, afterpulsing, timing jitter, and limited bandwidth [9], [10]. Currently, SNSPD is preferred for high-speed optical communications as it can detect single photons with high efficiency, making it well-suited for quantum communication applications. In recent years, there has been considerable interest in using SNSPDs for high-speed optical communication systems [11]. In 2013, the Lunar Laser Communications Demonstration (LLCD) project conducted by NASA demonstrated an optical communication system with 16-PPM and four 16-element SNSPD arrays. It achieved a world-record 3.48 photons/bit receiving sensitivity at a 622Mbps information rate [11].

Although SNSPD arrays can achieve high-speed information rates, the performance limit of a single SNSPD is unclear. This is due to the difficulty in analyzing the performance of high-speed optical PPM communication systems, which is caused by the dead time of an SNSPD [12]. While several attempts have been made to model PPM communication systems using an SNSPD, existing studies have not considered the fundamental case where the dead time of an SNSPD is longer than a PPM symbol time [13], [14]. In such cases, the detection of a symbol can be affected by the detection of its previous symbols due to the long dead time.

Several attempts have been made to model for PPM communication system using an SNSPD. The authors in [15] established the photon counting models and bit error rate (BER) model under the effect of the inter-slot interference. In [16] the authors proposed a BER model based on double generalized Gamma channel. BER performance modeling and analysis of a single-photon avalanche diodes (SPAD) optical receiver, which has similar the dead time characteristic with an SNSPD, is presented in [17].

Although extensive researches [15]–[18] have been carried out on low speed or simplified channel model, these studies did not consider the fundamental case that the dead time of an SNSPD is longer than a PPM symbol time. In such cases, the detection of a symbol would be affected by the detection of its previous symbols due to the long dead time [13], [14].

To the best of our knowledge, the performance analysis of high-speed PPM-SNSPD systems, where the SNSPD dead time is multiples of the PPM symbol time, is missed. Motivated by this, we investigate the performance of high-speed

This work was supported in part by the National Natural Science Foundation of China under contract No. 61971403, in part by the Strategic Priority Research Program of the Chinese Academy of Sciences, Grant No. XDA30030600.

laser PPM communication systems with an SNSPD, where the dead time of the SNSPD is multiple times the duration of a PPM symbol, denoted by N, where $N \geqslant 1$. In this work, we make the following contributions: (a) we analyze the error performance of high-speed PPM communication systems with an SNSPD using a Markov chain model to derive the photon detection probability for each time slot of the PPM symbol. We find that the probability of detecting one photon in the h-th slot is higher than that in the h'-th slot when $h > h'$, and(b) we derive closed-form expressions for the symbol error rate (SER) and channel coding rate of the system. Monte-Carlo simulation results of photon detection probability for each PPM time slot and system SER verify the correctness of our analysis.

II. Research Background of SNSPD using PPM

In this section, we will provide a brief overview of the operation mechanism of a superconducting nanowire single-photon detector (SNSPD) [19]. The classical hot spot model of the SNSPD, as described in [19], will be adopted for our analysis. The SNSPD consists of a superconducting nanowire and a sapphire substrate that participate in heat exchange during its operation [20]. To detect a single photon, the bias current of the nanowire must be less than the superconducting critical current, and the temperature of the nanowire must be less than the superconducting critical temperature. When an infrared photon disrupts hundreds of Cooper pairs, a hot spot is formed, and the superconducting state is broken. The hot spot expands along with joule heat generated by the superconducting nanowire. Once the superconducting state is broken, a spike pulse is generated. The rate of heat transfer to the sapphire substrate is faster than the rate of joule heat, causing the temperature of the superconducting nanowire to be reduced to that of the sapphire substrate [19]. Due to the reduction of the whole circuit, the recovery time is relatively long. The SNSPD cannot detect photons during the period when the superconducting current starts to decrease and fully recovers to the initial value. The duration of dead time T_d is the sum of pulse time and recovery time.

At extremely low optical power levels, the arrival of photons at the detector can be modeled as a Poisson process. The probability that n photons arrive at the detector within a time interval T_s, is given by the Poisson distribution:

$$p\left(n;\mu T_s\right) = \frac{\left(\mu T_s\right)^n e^{-\mu T_s}}{n!}, \tag{1}$$

where μ represents the average number of incident photons per second. Equ. 1 gives the probability of observing n photons within a time interval T_s, given the average photon arrival rate of μ.

In M-PPM, a symbol consists of M time slots, where only one slot carries an optical signal. This modulation scheme enhances anti-interference ability and improves optical peak power. The transmitted symbols are deterministically uniform, and in high-speed communication systems, the dead time is N times the symbol duration.

For a SNSPD with fixed T_d, it can only detect one photon in a PPM slot. The number of signal photons per slot is

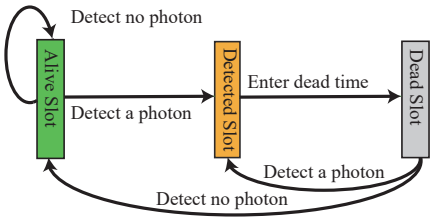

Fig. 1. The slot detection state for an SNSPD.

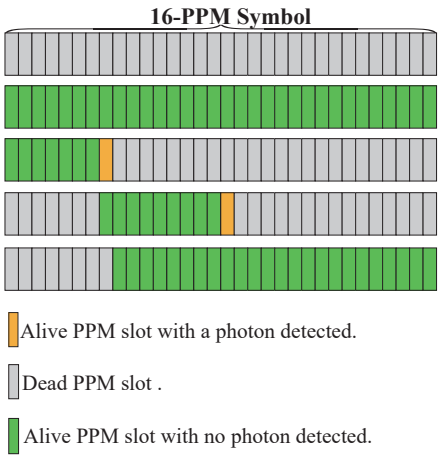

Fig. 2. The different symbol states for an SNSPD with 16-PPM.

denoted as n_s, and the number of background photons per slot is denoted as n_b. The photon counts in a time slot follow a Bernoulli distribution, given by

$$p(n) = \begin{cases} e^{-\mu T_s}, & n = 0, \\ 1 - e^{-\mu T_s}, & n = 1. \end{cases} \tag{2}$$

where $\mu T_s = n_s + n_b$ for a signal-slot, and $\mu T_s = n_b$ for a non-signal-slot. For simplicity, we let $p11 = p(1; n_s + n_b)$ and $p_{01} = p(0; n_s + n_b)$ while $p_{10} = p(1; n_b)$ and$p_{00} = p(0; n_b)$.

III. Error Performance of the Uncoded Systems

In this section, we analyze the performance of the PPM-SNSPD system with $T_d = N(MT_s)$. In particular, we model the SNSPD detector as a finite-state machine, and analyze the detection statistics using Markov chain. Eventually, we derive the SER of the uncoded PPM-SNSPD system as a function of ns, nb, and N. In addition, the achievable rate of the coded PPM-SNSPD is derived.

A. State transition

The photon detection behavior of an SNSPD can be modeled as a finite-state machine. Specifically, the states of an SNSPD can be characterized from two perspectives: slot detection states and symbol detection states. First, we introduce the slot detection states of an SNSPD, whose state transition graph is depicted in Fig. 1. We refer to the slots in which

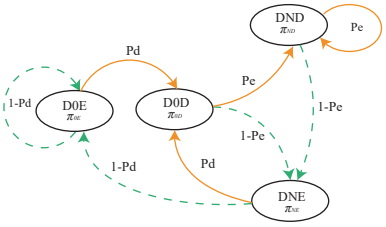

Fig. 3. States transition graph for the PPM symbols when $N = 1$.

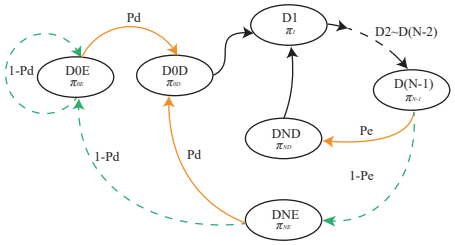

Fig. 4. States transition graph for the PPM symbols when $N > 1$.

the SNSPD can detect photon as alive slots. Each rectangle represents the detection state of an SNSPD in a time slot. The green one indicates that the SNSPD is alive but does not detect any photon. The yellow one indicates the PPM slot is alive with a photon detected. The gray one indicates that the SNSPD is dead. When the SNSPD is alive with no photon. detection, it will either stay in the same state or detect a photon in the next time slot. When the SNSPD detects a photon, it will be dead in the next time slot. The dead state will last for N symbol times.

Now, we consider the symbol detection states of an SNSPD. At symbol level, each photon detection of the SNSPD may affect the detection of N succeeding symbols. When the SNSPD detect a photon at slot-h, it would not react to the next $N-1$ symbols and the slots $0 \sim N-1$ of the N-th symbol. Therefore, the state transition at the symbol level is related to not only the position of the signal-slot, but also the relative duration of dead time N. We classify the behavior of the SNSPD into five symbol detection states depending on the feature of slot detection state transition during a symbol time. All possible detection states are depicted in Fig. 2. The states are defined as follows:

- D0E represents that the SNSPD is alive for all slot in the symbol time. In the next symbol time, the symbol state will stay in D0E or enter D0D.
- D0D represents that the SNSPD is alive at the start of current symbol time, and a photon is detected later. In the next symbol time, the SNSPD will go to D1 if $N > 1$, and will go to DND or DNE if $N = 1$.
- Di represents that the SNSPD is dead for the entire symbol time,$i = 1, ..., N-1$. The transition from D1 to D(N-1) are unidirectional because of the dead time.
- DNE represents that the slot resumes alive, but no photon is detected. In the next symbol time, the symbol state will enter D0E or D0D.
- DND represents that a photon is detected after the symbol is restored to the detection state. The SNSPD will enter D1 in the next symbol time.

First, we consider the state transition of an SNSPD with $N = 1$. The state transition graph is shown in Fig. 3. Because the dead time of SNSPD cannot last for a whole PPM symbol, Di does not exist. In the following, we will use the Markov chain to derive the steady-state probabilities of this SNSPD.

When the SNSPD is in D0E or DNE, it would be able to detect photon for all slots in the next symbol time. The probability of detecting a photon for an entirely detectable symbol is $P_d = 1 - e^{(n_s + n_b M)}$. When the SNSPD is in D0D or DND, it is dead at the beginning of next symbol time. The probability of detecting a photon in the next symbol time depends on when the SNSPD recovers from dead time. The average probability of detecting a photon for a partially detectable symbol time is denoted by P_e. The derivation of P_e would be presented later. We use $\boldsymbol{\pi} = [\pi_{0\mathrm{E}}, \pi_{0\mathrm{D}}, \pi_{1\mathrm{E}}, \pi_{1\mathrm{D}}]$ to represent the probability of each steady state in Fig. 3. The state transition matrix is as follows:

$$\mathbf{P} = \begin{array}{c} \\ \text{D0E} \\ \text{D0D} \\ \text{DNE} \\ \text{DND} \end{array} \begin{array}{c} \begin{array}{cccc} \text{D0E} & \text{D0D} & \text{DNE} & \text{DND} \end{array} \\ \begin{bmatrix} 1-P_d & P_d & 0 & 0 \\ 0 & 0 & 1-P_e & P_e \\ 1-P_d & P_d & 0 & 0 \\ 0 & 0 & 1-P_e & P_e \end{bmatrix} \end{array}. \tag{3}$$

According to steady-state conditions $\boldsymbol{\pi} P = \boldsymbol{\pi}$ and $\sum \boldsymbol{\pi} = 1$, the steady-state probability of each state can be expressed as a function of P_e and P_d:

$$\begin{cases} \pi_{0\mathrm{E}} = \dfrac{(1-P_d)(1-P_e)}{(1-P_e+P_d)} \\ \pi_{0\mathrm{D}} = \dfrac{P_d(1-P_e)}{(1-P_e+P_d)} \\ \pi_{1\mathrm{E}} = \dfrac{P_d(1-P_e)}{(1-P_e+P_d)} \\ \pi_{1\mathrm{D}} = \dfrac{P_d P_e}{(1-P_e+P_d)} \end{cases}. \tag{4}$$

The state transition graph for an SNSPD with $N > 1$ is shown in Fig. 4. Different from the state transition graph for $N = 1$, the state transition graph for $N > 1$ consists the entirely dead states D1 $\sim$ D(N-1). When the SNSPD is in D0D and DND, it will enter D1 in the next symbol time. We use $\boldsymbol{\pi} = [\pi_{0\mathrm{E}}, \pi_{0\mathrm{Dz}}, \pi_1, ..., \pi_{\text{N-1}}, \pi_{\mathrm{NE}}, \pi_{\mathrm{ND}}]$ to represent the probability of each state being steady in Fig. 4. The extended

state transition matrix is

$$\mathbf{P}=\begin{bmatrix} 1-P_d & P_d & 0 & 0 & 0 & \cdots & 0 & 0 & 0 \\ 0 & 0 & 1 & 0 & 0 & \cdots & 0 & 0 & 0 \\ 0 & 0 & 0 & 1 & 0 & \cdots & 0 & 0 & 0 \\ 0 & 0 & 0 & 0 & 1 & \cdots & 0 & 0 & 0 \\ \vdots & \vdots & \vdots & \vdots & \vdots & \ddots & \vdots & \vdots & \vdots \\ 0 & 0 & 0 & 0 & 0 & \cdots & 1 & 0 & 0 \\ 0 & 0 & 0 & 0 & 0 & \cdots & 0 & 1-P_e & P_e \\ 1-P_d & P_d & 0 & 0 & 0 & \cdots & 0 & 0 & 0 \\ 0 & 0 & 1 & 0 & 0 & \cdots & 0 & 0 & 0 \end{bmatrix}. \tag{5}$$

The steady-state probabilities are

$$\begin{cases} \pi_{\text{0E}}=\dfrac{(1-P_d)(1-P_e)}{(1-P_e+NP_d)} \\ \pi_{\text{0D}}=\dfrac{P_d(1-P_e)}{(1-P_e+NP_d)} \\ \pi_{\text{NE}}=\dfrac{P_d(1-P_e)}{(1-P_e+NP_d)} \\ \pi_{\text{ND}}=\dfrac{P_dP_e}{(1-P_e+NP_d)} \\ \pi_{\text{i}}=\dfrac{P_d}{(1-P_e+NP_d)} \end{cases}. \tag{6}$$

So far, the average probability of detecting a photon for a partially detectable symbol time P_e is unknown. Next, we will derive P_e so that the exact value of steady-state probabilities can be calculated.

B. Probability of Resuming

To derive P_e, we firstly need to know the probability that the SNSPD resumes at a give time slot. Let $P_r(h)$ represent the probability that the SNSPD return to detectable state in the h-th PPM slot. When the SNSPD detects a photon in slot h of the i-th symbol time, it will return to detectable state at slot h of the $(i+N)$-th symbol. Therefore,the probability that the SNSPD returns to detectable state is equivalent to the probability that a photon is detected in the h-th PPM slot. We can tell from Fig. 4 that photon detection occurs when the SNSPD is in D0D or DND. According to the total probability formula, $P_r(h)$ is

$$P_r(h)=\frac{\pi_{\text{0D}}P_1\{h\mid\pi_{\text{0D}}\}}{\pi_{\text{0D}}+\pi_{\text{ND}}}+\frac{\pi_{\text{ND}}P_1\{h\mid\pi_{\text{ND}}\}}{\pi_{\text{0D}}+\pi_{\text{ND}}}, \tag{7}$$

where $P_1\{h\mid\pi_{\text{0D}}\}$ and $P_1\{h\mid\pi_{\text{ND}}\}$ represent the probability that the SNSPD detects a photon in the h-th slot when it is in D0D and DND, respectively. They can be calculated using conditional probability formula as follows:

$$\begin{cases} P_1\{h\mid\pi_{\text{0D}}\}=\dfrac{A_h}{P_d} \\ P_1\{h\mid\pi_{\text{ND}}\}=\dfrac{\sum_{i=0}^{h}P_r(i)A_{h-i}}{P_e} \end{cases}. \tag{8}$$

The expression A_{h-i} represents the probability that a photon is detected at slot h when slot $0\sim$ slot $i-1$ are dead while slot $i\sim$ slot h are alive. Note that $A_{h-i}=A_{h'-i'}$ when $h-i=h'-i'$. It is given by

$$A_i=\left(\frac{i}{M}p_{00}^{i-1}p_{01}p_{10}+\frac{1}{M}p_{00}^{i}p_{11}+\frac{M-i-1}{M}p_{00}^{i}p_{10}\right). \tag{9}$$

By substituting (8) into (7), we can get

$$P_r(h)=\frac{(1-P_e)P_1\{h\mid\pi_{\text{0D}}\}}{P_d}+\sum_{i=0}^{h}P_r(i)P_1\{h-i\mid\pi_{\text{0D}}\}. \tag{10}$$

Equation (10) and $\sum_{i=0}^{M-1}P_r(i)=1$ form a system of linear equations in $M+1$ dimensions. $P_r(h)$ and P_e can be obtained.

C. Symbol Detection Probability and Transition Probability

With P_e known, we can calculate the steady-state probabilities $\boldsymbol{\pi}$. Now, we can derive the symbol detection probability $p_1(h)$, i.e. the probability that a photon is detected in the signal-slot.

There exist two states where the SNSPD detects a photon: D0D and DND. In the following, we derive the probability that detecting a photon at slot h in D0D and DND, respectively.

1) Considering that the SNSPD is in D0D, photon detection at slot h means that slot $0\sim$ slot h are all alive with no photon detected. Therefore, the probability of photon detection at slot h in the D0D state is $p_{00}^{h}p_{11}$.
2) In DND, the slot of the detector recovery need to be considered. The probability that slot $0\sim$ slot $(i-1)$ is in dead time is $\pi_{\text{(N-1)}}P_r(i)$. In this case, the probability that photon is detected in slot h is $p_{00}^{h-i}p_{11}$.

In summary, $p_1(h)$ can be expressed as

$$p_1(h)=\left(\underbrace{\pi_0p_{00}^{h}}_{Case1}+\underbrace{\pi_{(N-1)}\sum_{i=0}^{N}P_r(i)p_{00}^{h-i}}_{Case2}\right)p_{11}. \tag{11}$$

Now, we can obtain the symbol transition probability. Let $\mathcal{X}=\{\boldsymbol{x}_1,\ldots,\boldsymbol{x}_M\}$ be the input alphabet of the high-speed Poisson-SNSPD channel, where $\boldsymbol{x}_i=[x_{i,1},\ldots,x_{i,m}]$, $x_{i,i}=1$, $x_{i,j\neq i}=0$, Here, $\boldsymbol{x}_i$ represent the i-th PPM symbol, and x_{ij} specifies whether or not a pulse is emitted in the j-th time slot of that symbol. Let $\mathcal{Y}=\{\boldsymbol{y}_0,\boldsymbol{y}_1,\ldots,\boldsymbol{y}_M\}$ be the output alphabet of the channel, where $\boldsymbol{y}_0$ represents that no photon is detected during the entire symbol time, and $\boldsymbol{y}_i,(i=1,....,M)$ means that the i-th PPM symbol is received. The symbol transition probability $P_{ji}=P_{\mathbf{Y}|\mathbf{X}}\left(\boldsymbol{y}_j\mid\boldsymbol{x}_i\right)$ can be expressed by 12.

D. SER Performance of Uncoded PPM-SNSPD System

Knowing the symbol detection probability $p_1(h)$ and the steady state probabilities of an SNSPD, we can obtain the SER expression of the SNSPD. To be specific, there exist three types of receiving results in a symbol time. One is that no photon is detected in any slot. Since the preceding slot of PPM

$$P_{ji} = \begin{cases} 1 - \prod_{i=1}^{M-1} P_{ji}, & j = 0 \\ \omega_0 p_{00}^{j} p_{10} + \omega_{\text{(N-1)}} \left(\sum_{h=0}^{j} P_r(h) p_{00}^{j-h} \right) p_{10}, & j < i \\ \omega_0 p_{00}^{i} p_{11} + \omega_{\text{(N-1)}} \left(\sum_{h=0}^{i} P_r(h) p_{00}^{i-h} \right) p_{11}, & j = i \\ \omega_0 p_{00}^{j-1} p_{01} p_{10} + \omega_{\text{(N-1)}} \left(\sum_{h=0}^{i} P_r(h) p_{00}^{j-h-1} p_{01} p_{10} + \sum_{h=i+1}^{j} P_r(h) p_{00}^{j-h} p_{10} \right), & j > i \end{cases} \tag{12}$$

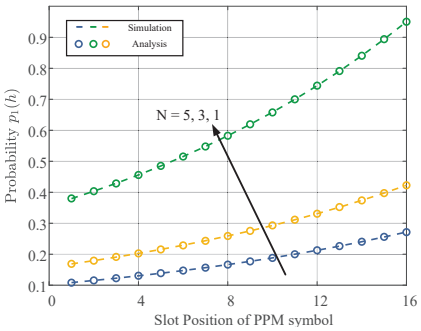

Fig. 5. Probability $p_1(h)$ for different the average signal photons per slot n_s when $n_b = 10^{-5}$ and $N = 3$.

symbols is more susceptible to information loss, we assume that the signal is transmitted in the first time slot when no photons are received. The probability of correct decoding is $\frac{p_{01}}{\sum_{i=1}^{M} p_{0i}}$. The other one is that a photon is detected in the signal-slot, and the probability of correct decoding is 1. The last one is that a photon is detected in an non-signal-slot, and the probability of correct decoding is 0. Therefore, SER is

$$P_s = 1 - \sum_{h\,=\,0}^{M-1} p_1\,(h) - \frac{(1 - \pi_{0D} - \pi_{ND})}{M}. \tag{13}$$

On average, a symbol error leads to $N_n = M \log_2 \frac{M}{2(M-1)}$ bit errors with binary mapping. Hence, the bit error probability after PPM demodulation can be estimated as $P_b = \frac{M}{2(M-1)} P_s$.

Performance limit of the coded PPM-SNSPD system Ideally, knowing the symbol transition probability, we can compute the channel capacity $C = \max_{Px} I(Y;X)$ of this system. However, our analysis show that SNSPD-PPM channel is not symmetric as the symbol detection probabilities are different when symbols are transmitted with equal probability $P_x = 1/M$. Hence, the SNSPD-PPM system can not reach the true capacity as $I(Y;X)|_{Px=1/M} < C$. In this case, achievable rate R_c (also called symmetric capacity) gives a more practical performance limit. To be specific, the achieve rate refers to the maximum code rate that can support reliable transmission with uniformly transmitted symbols, defined as

$$R_c = \frac{\mathbf{I}(\mathbf{X};\mathbf{Y})}{\sqrt{M}} \tag{14}$$

IV. Numerical Results

In this section, we present the numerical results from both analysis and simulation. First, we consider the performance under 16-PPM. In Fig. 5, we plot symbol detection probability p1(h) against the index of signal-slot h for different n_s. Our analysis and simulation fit closely. This verifies our analysis. For the same n_s, the detection probability will decrease as N increases. Overall, the detection probability decreases with the increment of N when n_s and n_b are constant. Essentially, it is observed that $p_1(h)$ increases with the index of time sloth. The slots at the back of the PPM symbol time are more likely to detect a photon from pulse. The detection probability of the last slot is almost three times that of the first slot in PPM symbol when $n_s = 5$. This is because the symbol detection of front slots is more likely to be erased by dead time. For instance, consider that the SNSPD resumes in slot h', when signal-slot h is before slot h', this symbol would not be successfully detected. In consequences, the signal-slots in the front of a PPM symbol time have a lower detection probability than the signal-slots in the rear. Such a detection characteristics makes the channel asymmetric. Modulation shaping technique, such as pulse shaping and probabilistic shaping, might be used for improving the error performance of such an asymmetric channel.

Fig. 6 demonstrate the SER performance for various noise intensity no. The SER decreases with ns until an error floor is reached. This is due to the fact that the detection error is jointly affected by the detection probability of signal-slot, noise intensity, and the dead time. When ns is low, the probability of a successful photon detection p_{11} increases with n_s. Therefore, SER decreases with increasing n_s. When p_{11} approaches 1, the error is dominated by noise and dead time, which are both constant for each SER curve, so the SER reaches the error floor. At this stage, it is inefficient to improve signal power at transmitter as it only brings minor SER improvement. On the other hand, the SER level at error floor decreases if either n or N reduces. This suggests that given an SNSPD with a constant dead time Ta, the error floor could be diminished by slowing down transmission rate, which reduces N. Of course, parallel SNSPD arrays could be used for achieving a satisfying SER while maintaining a high transmission rates because it diminishes the probability that photon detection is blocked by dead time.

Fig. 7 demonstrates the achievable rate Rc for various PPM order M when $N = 1$. In particular, we consider a constant symbol time T such that $T_s = T/M$, and $n_b = \mu T/M$. For each PPM order, the achievable rate rises with Pavg till it reaches a upper constraint, while a lower PPM order gives a higher rate constrain. For a constant code rate R_c below 0.6, a higher PPM order brings a higher energy efficiency such that less average transmission power is required to provides

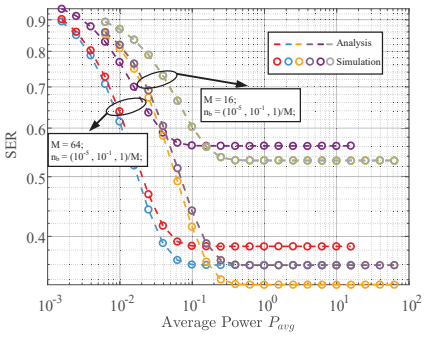

Fig. 6. SER of 16-PPM with different noise power when $N = 1$.

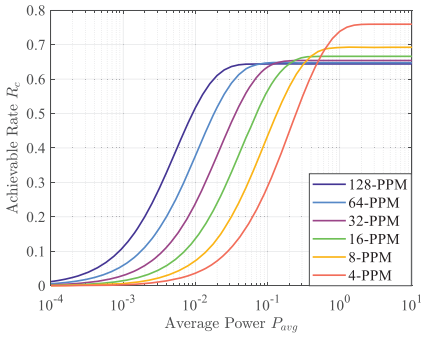

Fig. 7. SER of 16-PPM with different N when $n_b = 10^{-5}$.

reliable transmission at rate R_c.

V. Conclusion

In this paper, we investigate the performance of a high-speed PPM-SNSPD communication system, where a single SNSPD is used. The SER of the uncoded PPM-SNSPD system as well as the achievable rate of the coded PPM-SNSPD system are derived.In such a high-speed system, the dead time of the SNSPD is multiple times of a PPM symbol time. As a result, the photon detection probability of each PPM time slot depends on the state of the SNSPD since a photon detection event blocking the detection of photons in the following several PPM symbols. Based on the photon detection probability for each PPM time slot, the closed-from expressions for the SER of the uncoded system was derived. The analysis shows that the PPM-SNSPD system has a detection limit such that SER would not decrease with increasing signal intensity n_s. In other words, this system has an error floor associated with n_s, n_b, and N. With our derived SER expression, we can calculate the most efficient transmission power given n_b and N. Knowing that equipping SNSPD array can effetively improve the photon detection efficiency. In the further, we aim to analyze the performance of the high-speed PPM systems with an SNSPD array base on our analysis presented in this paper. It is also worth to note that the symbol detection probability analysis shows that the PPM-SNSPD channel is asymmetric. Hence, we compute the achievable rate of the system to gives a practical performance limit for this system. The observation on channel asymmetry suggest that we can investigate modulation shaping techniques to the PPM-SNSPD system for potential performance improvement.

References

[1] H. Hemmati, *Deep space optical communications*. John Wiley & Sons, 2006.

[2] Z. Shi, W. Wang, X. Wu, and L. Yang, "A technique for measuring dynamic slot-power of optical PPM signals based on SNSPD," *IEEE Photon. Technol. Lett.*, 2022.

[3] G. Wen, J. Huang, J. Dai, L. Zhang, and J. Wang, "Performance analysis optimization and experimental verification of a photon-counting communication system based on non-photon-number-resolution detectors," *Optics Communications*, vol. 468, p. 125771, 2020.

[4] S. G. Wilson, M. Brandt-Pearce, M. Baedke, and Q. Cao, "Optical MIMO transmission with multipulse PPM," in *International Symposium on Information Theory*, 2004.

[5] M. Charbit and C. Bendjaballah, "Probability of error and capacity of PPM photon counting channel," *IEEE Trans. Commun.*, vol. 34, no. 6, pp. 600–605, 1986.

[6] J. Pierce, "Optical channels: Practical limits with photon counting," *IEEE Trans. Commun.*, vol. 26, no. 12, pp. 1819–1821, 1978.

[7] K. Chakraborty and P. Narayan, "The Poisson fading channel," *IEEE Trans. Inf. Theory*, vol. 53, no. 7, pp. 2349–2364, 2007.

[8] Y. Yamamoto and H. Haus, "Preparation, measurement and information capacity of optical quantum states," *Reviews of Modern Physics*, vol. 58, no. 4, p. 1001, 1986.

[9] B. Edwards, "Overview of the Mars laser communications demonstration project," in *AIAA Space 2003 Conference & Exposition*, 2003, p. 6417.

[10] B. S. Robinson, A. J. Kerman, E. A. Dauler, R. J. Barron, D. O. Caplan, M. L. Stevens, J. J. Carney, S. A. Hamilton, J. K. Yang, and K. K. Berggren, "781 Mbit/s photon-counting optical communications using a superconducting nanowire detector," *Optics letters*, vol. 31, no. 4, pp. 444–446, 2006.

[11] C. M. Natarajan, M. G. Tanner, and R. H. Hadfield, "Superconducting nanowire single-photon detectors: physics and applications," *Superconductor ence Technology*, vol. 25, no. 6, pp. 63 001–63 016(16), 2012.

[12] D. Caplan, "High-performance free-space laser communications and future trends," in *Optical Amplifiers and Their Applications*. Optica Publishing Group, 2005, p. TuB1.

[13] E. Sarbazi and H. Haas, "Detection statistics and error performance of SPAD-based optical receivers," in *2015 IEEE 26th Annual International Symposium on Personal, Indoor, and Mobile Radio Communications (PIMRC)*. IEEE, 2015, pp. 830–834.

[14] E. Sarbazi, M. Safari, and H. Haas, "The impact of long dead time on the photocount distribution of SPAD receivers," in *2018 IEEE Global Communications Conference (GLOBECOM)*. IEEE, 2018, pp. 1–6.

[15] Y. Mu, C. Wang, Y.-b. Xu, X.-x. Du, Q.-y. Pan, H.-y. Zhang, and Y.-j. Zhu, "Time-coordinated SPAD-based receiver for high-speed optical wireless communication," *Optics Communications*, vol. 526, p. 128706, 2023.

[16] B. Li, S. Tong, H. Yao, L. Zhang, and Y. Liu, "BER analysis of a deep space optical communication system based on snspd over double generalized gamma channel," *IEEE Photonics Journal*, vol. 10, pp. 1–1, 2018.

[17] H. Mahmoudi, M. Hofbauer, B. Steindl, K. Schneider-Hornstein, and H. Zimmermann, "Modeling and analysis of BER performance in a spad-based integrated fiber optical receiver," *IEEE Photonics Journal*, vol. PP, no. 99, pp. 1–1, 2018.

[18] H. Ivanov, E. Leitgeb, and G. Freiberger, "Characterization of Poisson channel for deep space FSO based on SNSPD technology by experimental demonstration," in *2018 11th International Symposium on Communication Systems, Networks & Digital Signal Processing (CSNDSP)*. IEEE, 2018, pp. 1–5.

[19] C. M. Natarajan, M. G. Tanner, and R. H. Hadfield, "Superconducting nanowire single-photon detectors: physics and applications," *Superconductor science and technology*, vol. 25, no. 6, p. 063001, 2012.

[20] J. Yang, A. J. Kerman, E. A. Dauler, V. Anant, K. M. Rosfjord, and K. K. Berggren, "Modeling the electrical and thermal response of superconducting nanowire single-photon detectors," *IEEE Trans. Appl. Supercond.*, vol. 17, no. 2, pp. 581–585, 2007.